International Journal of Heat and Mass Transfer 51 (2008) 5777–5784

Contents lists available at ScienceDirect

International Journal of Heat and Mass Transfer

journal homepage: www.elsevier.com/locate/ijhmt

Mixed convection with heating effects in a vertical porous annulus with a radially varying magnetic field

A. Barletta [a], S. Lazzari [a], E. Magyari [b], I. Pop [c,*]

[a] Dipartimento di Ingegneria Energetica, Nucleare e del Controllo Ambientale (DIENCA), Università di Bologna, Via dei Colli 16, I-40136 Bologna, Italy
[b] Institut für Hochbautechnik, ETH, Zürich, Wolfgang-Pauli-Str. 1, CH-8093 Zürich, Switzerland
[c] Faculty of Mathematics, University of Cluj, R-3400 Cluj, CP 253, Romania

ARTICLE INFO

Article history:
Received 20 May 2008
Available online 28 July 2008

Keywords:
Mixed convection
Fully developed regime
MHD flow
Porous medium
Darcy law
Analytical solution

ABSTRACT

Fully developed parallel flow in an annular region filled with a porous medium surrounding an electric cable is investigated. The effects of buoyancy and MHD force as well as the heat generation due to Joule heating and viscous dissipation are taken into account. The mixed convection seepage flow is analyzed according to Darcy law and to Boussinesq approximation. Buoyancy effect is modelled by setting the isoflux wall temperature as the reference temperature. As a consequence of this choice, the local momentum and energy balance equations and the boundary conditions can be written in a dimensionless form that defines an initial value problem instead of a boundary value problem. The initial value problem is solved both by an analytical series method and by numerical integration. The effect of the radially varying magnetic field on the fluid velocity and temperature distributions is analyzed. It is shown that a significantly strong magnetic force tends to inhibit the flow even for a high hydrodynamic pressure gradient.

1. Introduction

The effects of an external magnetic field on convection flows in porous media has gained through the years an increasing attention, as pointed out in the comprehensive review by Nield and Bejan [1]. The interest in this field is due to the wide range of applications either in engineering and in geophysics, such as the optimization of the solidification processes of metals and metal alloys, the study of geothermal sources, the treatment of nuclear fuel debris, the control of underground spreading of chemical wastes and pollutants and the design of MHD power generators.

The analysis of hydromagnetic flows in porous media has been the subject of several recent papers [2–14]. These investigations can be considered as theoretical extensions of the deep knowledge reached in the last decades regarding MHD effects in fluid dynamics and convection heat transfer.

Most of the published papers on convection and porous media under the action of a magnetic field deal with external flows and consider cases such that the magnetic field is uniform. Kumari et al. [3] employ the numerical Keller box method to study the mixed convection in a porous medium around a vertical wedge. The boundary layer equations are solved by these authors considering the Brinkman model with inertia term for momentum transport and by taking into account both the effects of Joule heating and viscous dissipation in the energy balance. Chamkha and Quadri [4] consider hydromagnetic natural convection from a horizontal permeable cylinder and obtain a numerical solution of the non-similar boundary layer problem by using a finite difference method. El-Amin [7] investigates external free convection from either a horizontal plate or a vertical plate with uniform heat flux. The local balance equations are written with reference to power-law fluid flow in a porous medium, transformed introducing a similarity variable and solved through a fourth-order Runge–Kutta method with shooting technique. Postelnicu [8] analyzes simultaneous heat and mass transfer by natural convection from a vertical flat plate with uniform temperature in an electrically conducting fluid saturated porous medium. This author uses the Darcy–Boussinesq model including Soret and Dufour effects and solves numerically the similar boundary layer equations.

An interesting research work on analytical solutions for MHD effects in heat and momentum transfer involving either Newtonian or non-Newtonian fluids has been recently performed by Hayat and coworkers [10–12]. For instance, in Hayat et al. [10], the authors obtain exact solution for the MHD pipe flow of a Burgers' fluid in a porous medium by means of Fourier transform method. These authors adopt a modified Darcy's relationship and treat as special cases Oldroyd-B, Maxwell, second grade and Navier–Stokes fluid models. In a very recent paper, Khan et al. [11] treat incompressible Oldroyd-B fluid transient flow in a porous duct of rectangular cross-section, in the presence of an applied uniform magnetic field normal to the flow direction.

* Corresponding author.
E-mail address: pop.ioan@yahoo.co.uk (I. Pop).

0017-9310/$ - see front matter © 2008 Elsevier Ltd. All rights reserved.
doi:10.1016/j.ijheatmasstransfer.2008.05.018

Nomenclature

$A_n, \widetilde{A}_n, B_n, G_n$	series coefficients
$\mathbf{B}$	magnetic field
B_0	constant magnetic field, Eq. (1)
Br	Brinkman number, Eq. (11)
$\hat{\mathbf{e}}_\theta, \hat{\mathbf{e}}_Z$	angular and axial unit vectors
$\mathbf{g}$	gravitational acceleration
g	modulus of the gravitational acceleration
$G(r)$	dimensionless function, Eq. (32)
Gr	Grashof number, Eq. (11)
I	electric current
k	thermal conductivity of the fluid
K	permeability
K_{eff}	effective permeability, Eq. (7)
Li_2	Euler's dilogarithm function
M	Hartmann number, Eq. (8)
Nu	Nusselt number, Eq. (18)
p	pressure
P	hydrodynamic pressure, $p + \rho g Z$
q_{w}	heat flux at the internal wall
r	dimensionless radial coordinate, Eq. (11)
R	radial coordinate
R_1	internal radius
R_2	external radius
Re	Reynolds number, Eq. (11)
t	dimensionless temperature, Eq. (11)
T	temperature
T_{ref}	reference temperature, Eq. (4)
T_{w}	temperature of the external boundary
$u, \tilde{u}$	dimensionless velocity, Eqs. (11) and (43)
$u_{\mathrm{m}}, \tilde{u}_{\mathrm{m}}$	dimensionless average velocity, Eq. (20) and (43)
$\mathbf{U}$	velocity
U	axial velocity component
U_{m}	average velocity in a transverse cross-section, Eq. (19)
U_{ref}	reference velocity, Eq. (13)
Z	axial coordinate

Greek symbols

β	volumetric coefficient of thermal expansion
γ	radial aspect ratio, Eq. (11)
ΔT	reference temperature difference, Eq. (12)
η	dynamic viscosity
θ	angular coordinate
Λ	dimensionless parameter, Eq. (43)
μ_0	magnetic permeability of vacuum
Ξ	dimensionless parameter, Eq. (11)
ρ	mass density
σ	electric conductivity of the fluid
ϕ	porosity

Bhadauria [13] analyzes the thermal instability of Brinkman model flow in an electrically conducting fluid saturated porous medium confined between two horizontal walls. The presence of an applied vertical magnetic field and uniform rotation around a vertical axis are considered.

In the present paper, we will study a physically conceivable system sufficiently simple to be described by a completely analytical solution of the governing equations. In the literature, the main value of analytical solutions is that they can be used as benchmarks to test numerical codes designed to study actual industrial devices, usually too complicated to be described by an analytical solution. There is also a second important value of analytical solutions: their simple and basic character allows one to investigate the fundamental aspects of a given physical phenomenon.

The aim of the present paper is to perform a study of combined forced and free flow of an electrically conducting fluid in a vertical annular porous medium surrounding a straight cylindrical electric cable. For instance, a technical system that can be approximately described according to this model is an electric cable surrounded by moist soil, especially in the case where salt water is present. The cable generates a transverse radially varying magnetic field in the fluid and yields to the fluid saturated porous medium a uniform heat input through the internal boundary of the annulus. Thus, the analysis will refer to an internal flow and to a non-uniform magnetic field. The Darcy–Boussinesq model is considered and the non-linear equations will be solved both analytically with a power series method and numerically by predictor–corrector Adams method.

2. Mathematical model

Let us consider a fluid saturated vertical porous annulus with internal radius R_1 and external radius R_2, that surrounds a very long straight cable with radius R_1 carrying a constant electric current I (see Fig. 1). Let us assume that the cable is electrically insulated and that the magnetic field created by the current I is not appreciably modified by the feedback field induced by the fluid flow in the porous medium. The fluid flow in the porous medium is steady, laminar, parallel and fully developed, so that the seepage velocity can be expressed as $\mathbf{U} = U\hat{\mathbf{e}}_Z$, where $\hat{\mathbf{e}}_Z$ is the unit vector in the axial direction Z. Biot–Savart law implies that the magnetic field $\mathbf{B}$ generated by the electric current I is given by

$$\mathbf{B} = B_0 \frac{R_1}{R}\hat{\mathbf{e}}_\theta, \quad B_0 = \frac{\mu_0 I}{2\pi R_1}, \tag{1}$$

where $\hat{\mathbf{e}}_\theta$ is the unit vector in the azimuthal direction θ. The flow in the porous medium is described according to Darcy law and the effect of buoyancy is considered through the Boussinesq approximation [1,15]. Therefore, the mass balance equation requiring $\mathbf{U}$ to be

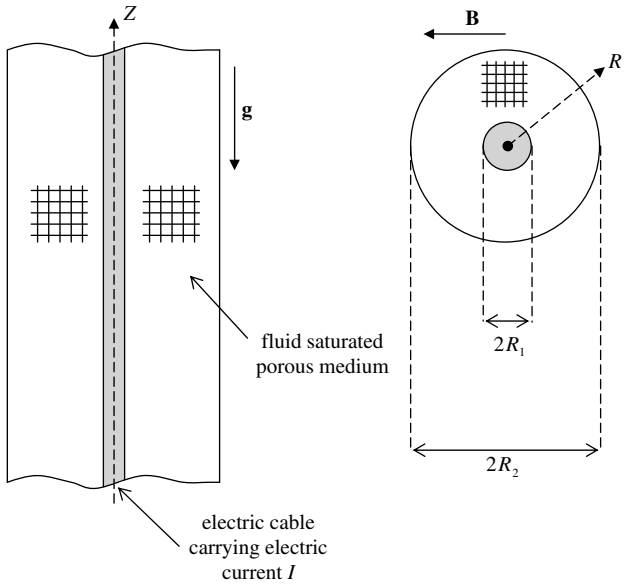

Fig. 1. Drawing of the vertical annulus.

solenoidal implies that $U = U(R)$, while the momentum balance in the Z, R and θ directions yields

$$\frac{\eta}{K}U = -\frac{\sigma B_0^2}{\phi}\frac{R_1^2}{R^2}U + \rho\beta g(T - T_{\rm ref}) - \frac{\partial P}{\partial Z}, \tag{2}$$

$$\frac{\partial P}{\partial R} = 0, \quad \frac{\partial P}{\partial \theta} = 0, \tag{3}$$

where the hydrodynamic pressure $P = p + \rho g Z$ is the difference between the pressure p and the hydrostatic pressure $-\rho g Z$. Eq. (3) imply that $P = P(Z)$. In analogy with Morton's treatment [16], the reference temperature $T_{\rm ref}$ introduced in the buoyancy term is chosen as the fluid temperature at the heated boundary $R = R_1$, namely

$$T_{\rm ref} = T|_{R=R_1}. \tag{4}$$

Note that the MHD body force appearing on the right hand side of Eq. (2) is evaluated, as suggested by Nield [17], considering the intrinsic velocity $\mathbf{U}/\phi$ instead of the seepage velocity $\mathbf{U}$. In fact, according to the Dupuit–Forchheimer relation, the intrinsic velocity is the ratio between the seepage velocity and the porosity ϕ.

The inner boundary of the porous medium, $R = R_1$, is subject to a uniform wall heat flux $q_{\rm w}$ due to the Joule heat generation inside the electric cable. The outer boundary, $R = R_2$, is assumed to be isothermal at temperature $T_{\rm w}$. If the axial length of the annular porous medium is much greater than R_2, then it is reasonable to assume a purely radial heat flow, *i.e.* a temperature field T depending only on R. As a consequence, Eq. (2) implies that $\mathrm{d}P/\mathrm{d}Z$ is independent of Z. Then, the local energy balance in steady regime for the fluid saturated porous medium can be expressed as

$$\frac{k}{R}\frac{\mathrm{d}}{\mathrm{d}R}\left(R\frac{\mathrm{d}T}{\mathrm{d}R}\right) + \frac{\sigma B_0^2}{\phi^2}\frac{R_1^2}{R^2}U^2 + \frac{\eta}{K}U^2 = 0. \tag{5}$$

The thermal boundary conditions are given by

$$-k\left.\frac{\mathrm{d}T}{\mathrm{d}R}\right|_{R=R_1} = q_{\rm w}, \quad T(R_2) = T_{\rm w}. \tag{6}$$

In Eq. (5), the second and the third term on the right hand side represent the Joule heating and the viscous dissipation contributions, respectively.

Eq. (2) would suggest that the effect of the external magnetic field may be dealt with by a proper definition of a radially varying *effective permeability* [17],

$$K_{\rm eff} = K\left(1 + \frac{\sigma B_0^2 R_1^2 K}{\eta\phi R^2}\right)^{-1}. \tag{7}$$

However, if the heat generation contributions appearing in the energy balance Eq. (5) are non-negligible, then the effective permeability is no more a convenient definition in order to deal with the magnetic field terms in the balance equations. This circumstance is due to the ϕ^{-2} term in the Joule heating contribution instead of the ϕ^{-1} term appearing in the definition of effective permeability, Eq. (7). In other words, the present MHD flow problem cannot be reduced to an equivalent porous flow problem with a properly defined effective permeability $K_{\rm eff}$ and without MHD effects, except for the limiting case of negligible heat generation contributions in the energy balance.

One can define a modified Hartmann number, M, such that

$$M^2 = \frac{\sigma B_0^2 K}{\eta\phi}. \tag{8}$$

Then, Eqs. (2) and (5) can be rewritten as

$$\frac{\eta}{K}\left(1 + \frac{M^2 R_1^2}{R^2}\right)U = \rho\beta g(T - T_{\rm ref}) - \frac{\mathrm{d}P}{\mathrm{d}Z}, \tag{9}$$

$$\frac{k}{R}\frac{\mathrm{d}}{\mathrm{d}R}\left(R\frac{\mathrm{d}T}{\mathrm{d}R}\right) + \frac{\eta}{K}\left(1 + \frac{M^2 R_1^2}{\phi R^2}\right)U^2 = 0. \tag{10}$$

2.1. Definition of the modified Hartmann number for MHD Darcy flows

The governing parameter that determines the strength of the magnetic effects on the velocity and temperature field is the modified Hartmann number M. More precisely, its definition given by Eq. (8) is an adjustment for porous media of the classical definition of Hartmann number given for clear fluids [18]. Eq. (8) points out that a high value of M does not only imply a high magnetic field, but also a fluid with high electric conductivity and low viscosity, as well as a medium with a high permeability to porosity ratio. Highly conductive fluids such as liquid metals yield large values of the ratio σ/η. On the other hand, the ratio K/ϕ strongly depends on the structure of the solid matrix. If one refers to mercury around 20 °C, one has $\sigma/\eta \approx 10^9\ \Omega^{-1}\ \mathrm{N}^{-1}$ [18]. The ratio K/ϕ can reasonably reach values of the order of $10^{-7}\ \mathrm{m}^2$ [19]. As a consequence, conditions may occur such that $\sigma K/(\eta\phi) \approx 10^2\ \mathrm{T}^{-2}$. This means that values of M of order 1 can be reached with $B_0 \approx 10^{-1}$ T that is certainly a very strong magnetic field, although perfectly feasible in practice. As it will be discussed in the following sections, a value of M of order 1 is characteristic of an important MHD effect in Darcy flow. Significantly higher values of M yield, in the flow problem under exam, to a system saturation. Indeed, the damping effect of the magnetic field on the fluid velocity becomes so strong that the fluid is almost brought to a rest state. Therefore, although decidedly hard to be obtained in the laboratory, values of M such as 8 or even 10^3 will be considered in the following discussion only in order to evidence this saturation effect, *i.e.* in order to compare these cases with the limit $M \to \infty$.

2.2. Dimensionless quantities

Let us define the dimensionless quantities

$$r = \frac{R}{R_1}, \quad u = \frac{U}{U_{\rm ref}}, \quad t = \frac{T - T_{\rm ref}}{\Delta T}, \quad \gamma = \frac{R_2}{R_1},$$
$$Gr = \frac{\rho^2\beta g\Delta T K R_1}{\eta^2}, \quad Re = \frac{\rho U_{\rm ref} R_1}{\eta},$$
$$\Xi = \frac{Gr}{Re} = \frac{\rho\beta g K\Delta T}{\eta U_{\rm ref}}, \quad Br = \frac{\eta U_{\rm ref}^2 R_1^2}{kK\Delta T}, \tag{11}$$

where ΔT and $U_{\rm ref}$ are, respectively, the reference temperature difference and the reference velocity given by

$$\Delta T = \frac{q_{\rm w} R_1}{k}, \tag{12}$$

$$U_{\rm ref} = -\frac{K}{\eta}\frac{\mathrm{d}P}{\mathrm{d}Z}. \tag{13}$$

The dimensionless parameters Gr, Re and Br represent respectively the modified Grashof, Reynolds and Brinkman numbers. It must be mentioned that Eq. (11) implies that $1 \leqslant r \leqslant \gamma$. On account of Eqs. (11)–(13), the governing Eqs. (9) and (10) can be rewritten as

$$\left(1 + \frac{M^2}{r^2}\right)u = \Xi t + 1, \tag{14}$$

$$\frac{1}{r}\frac{\mathrm{d}}{\mathrm{d}r}\left(r\frac{\mathrm{d}t}{\mathrm{d}r}\right) + Br\left(1 + \frac{M^2}{\phi r^2}\right)u^2 = 0, \tag{15}$$

while the first thermal boundary condition (6) yield

$$\left.\frac{\mathrm{d}t}{\mathrm{d}r}\right|_{r=1} = -1. \tag{16}$$

Eqs. (4) and (11) provide an additional constraint on the dimensionless temperature t, namely

$$t(1) = 0. \tag{17}$$

The input dimensionless parameters needed to solve Eqs. (14)–(17) are: the porosity ϕ, the Hartmann number M, the aspect ratio γ, the Brinkman number Br, the ratio Ξ between the Grashof number Gr and the Reynolds number Re.

The definition of the dimensionless temperature t given in Eq. (11) contains the difference $T(R) - T(R_1)$. In fact, the natural input parameter is not the temperature $T(R_1)$ of the isoflux wall, but the temperature T_w of the isothermal wall $R = R_2$. However, after having determined the solution of Eqs. (14)–(17), the value of $T(R_1) = T_{ref}$ can be easily obtained as $T(R_1) = T_w - t(\gamma)\Delta T$.

It must be pointed out that the Brinkman number Br represents an overall factor of the heat generation terms in the dimensionless energy balance Eq. (15). Thus, the limit $Br \to 0$ determines the special case where both the viscous dissipation effect and the Joule heating contribution are negligible.

2.3. Nusselt number and flow rate parameter

The heat transfer from the heated boundary $R = R_1$ to the cooled isothermal boundary $R = R_2$ is described through the Nusselt number defined as

$$Nu = \frac{q_w R_1}{k[T(R_1) - T_w]} = -\frac{1}{t(\gamma)}. \tag{18}$$

Another technically interesting quantity is the ratio between the average velocity in a transverse cross-section,

$$U_m = \frac{2}{R_2^2 - R_1^2}\int_{R_1}^{R_2} U R\,\mathrm{d}R, \tag{19}$$

and the reference velocity U_{ref}, namely

$$u_m = \frac{U_m}{U_{ref}} = \frac{2}{\gamma^2 - 1}\int_1^{\gamma} u r\,\mathrm{d}r. \tag{20}$$

The flow rate parameter u_m allows one to obtain the relation between the average velocity U_m and the vertical pressure gradient $\mathrm{d}P/\mathrm{d}Z$, as shown by Eqs. (13) and (20). In fact, one easily obtains the relation

$$U_m = -\frac{u_m K}{\eta}\frac{\mathrm{d}P}{\mathrm{d}Z}. \tag{21}$$

3. Solution procedure

3.1. Special cases

In the following limiting cases, closed form solutions of Eqs. (14)–(17) exist.

3.1.1. Limit $Br \to 0$

If $Br \to 0$, *i.e.* if the internal heat generation effects are negligible, one obtains

$$t(r) = -\ln(r), \tag{22}$$

$$u(r) = \frac{r^2}{r^2 + M^2}[1 - \Xi \ln(r)]. \tag{23}$$

- A special subcase is forced convection flow ($\Xi \to 0$) where

$$u(r) = \frac{r^2}{r^2 + M^2}. \tag{24}$$

- Another special subcase is the limit of vanishing pressure gradient, $\mathrm{d}P/\mathrm{d}Z \to 0$. This limit corresponds to a flow driven only by buoyancy force and by MHD body force, and represents the MHD free convection regime,

$$\lim_{\Xi\to\infty}\frac{u(r)}{\Xi} = -\frac{r^2\ln(r)}{r^2 + M^2}. \tag{25}$$

- Finally, a third special subcase is represented by the limit of negligible MHD body force, $M \to 0$,

$$u(r) = 1 - \Xi \ln(r). \tag{26}$$

3.1.2. Limit $\Xi \to 0$

In forced convection regime, *i.e.* if $\Xi \to 0$, $u(r)$ is still given by Eq. (24), whatever is the value of Br, while $t(r)$ is given by

$$\begin{aligned} t(r) &= -\ln(r) - \frac{Br}{\phi}\int_1^r \frac{\bar{r}^3(\phi\bar{r}^2 + M^2)}{(\bar{r}^2 + M^2)^2}\ln\left(\frac{r}{\bar{r}}\right)\mathrm{d}\bar{r} \\ &= -\ln(r) + \frac{Br}{4\phi(M^2+1)}\Big\{2[\phi + M^2(2\phi - 1) + 2M^2(M^2+1) \\ &\quad \times (2\phi - 1)\ln(M)]\ln(r) - M^2(M^2+1)\ln(M^2+1) \\ &\quad \times [1 - \phi + 2(2\phi - 1)\ln(r)] - (M^2+1)[(r^2 - 1)\phi \\ &\quad + M^2(\phi - 1)\ln(M^2 + r^2)] - M^2(M^2+1)(2\phi - 1) \\ &\quad \times \left[Li_2\left(-\frac{r^2}{M^2}\right) - Li_2\left(-\frac{1}{M^2}\right)\right]\Big\}, \end{aligned} \tag{27}$$

where $Li_2(z)$ is Euler's dilogarithm function defined as [20],

$$Li_2(z) = \sum_{n=1}^{\infty}\frac{z^n}{n^2}. \tag{28}$$

In the limit $M \to 0$, one obtains in this case

$$t(r) = \frac{1}{4}[Br(1 - r^2) + 2(Br - 2)\ln(r)]. \tag{29}$$

3.1.3. Limit $M \to \infty$

An interesting limiting case is that of a very large MHD force. This limit, in the dimensionless Eqs. (14)–(17), is mathematically expressed as $M \to \infty$. If one takes $M \to \infty$ in Eq. (14), then one obtains $u = 0$, whatever is the value of Ξ. Moreover, by substituting $u = 0$ in Eq. (15) and by considering the conditions (16) and (17), one obtains the logarithmic profile of the dimensionless temperature $t(r)$ given by Eq. (22). In other words, a very large magnetic field forces the fluid to be at rest, even if a vertical hydrodynamic pressure gradient is applied. As a consequence, no heat generation either due to viscous dissipation or to Joule heating occurs in the porous medium. Then, the annular porous layer around the cable thermally behaves as a solid and the temperature field is that of pure conduction.

3.2. The general power series solution

As a consequence of Eq. (14), the dimensionless governing Eqs. (15)–(17) imply an initial value problem for the dimensionless temperature t, namely

$$rt''(r) + t'(r) + BrG(r)[\Xi t(r) + 1]^2 = 0, \tag{30}$$

$$t(1) = 0, \quad t'(1) = -1, \tag{31}$$

where

$$G(r) = \frac{r^3(\phi r^2 + M^2)}{\phi(r^2 + M^2)^2}. \tag{32}$$

In Eqs. (30) and (31), as well as in the following, primes are used to denote differentiation with respect to r.

A convenient procedure to solve the initial value problem given by Eqs. (30) and (31) is based on a power series expansion of $t(r)$ around $r = 1$,

$$t(r) = \sum_{n=0}^{\infty} A_n (r-1)^n. \tag{33}$$

On account of Eq. (31), the coefficients A_0 and A_1 are easily obtained

$$A_0 = 0, \quad A_1 = -1. \tag{34}$$

From Eq. (32), the power series expansion of $G(r)$ around $r = 1$ is given by

$$G(r) = \sum_{n=0}^{\infty} G_n (r-1)^n, \tag{35}$$

where

$$G_0 = \frac{M^2+\phi}{\phi(M^2+1)^2}, \quad G_1 = \frac{3M^4+(5\phi-1)M^2+\phi}{\phi(M^2+1)^3},$$
$$G_2 = \frac{M^2[3M^4+2(5\phi-4)M^2-2\phi+1]}{\phi(M^2+1)^4},$$
$$G_3 = \frac{M^2[M^6+5(2\phi-3)M^4-5(4\phi-3)M^2+2\phi-1]}{\phi(M^2+1)^5}, \ldots \tag{36}$$

By substituting Eqs. (33) and (35) into Eq. (30), one obtains a recursive relation for the coefficients A_n with $n \geqslant 2$,

$$A_{n+2} = -\frac{n+1}{n+2} A_{n+1} - \frac{Br}{(n+1)(n+2)} \times \left[\Xi^2 \sum_{j=0}^{n} G_{n-j} \left(\sum_{i=0}^{j} A_i A_{j-i} \right) + 2\Xi \sum_{j=0}^{n} G_{n-j} A_j + G_n \right]. \tag{37}$$

The first coefficients obtained through this recursive relation are

$$A_2 = \frac{1}{2}(1 - BrG_0), \quad A_3 = \frac{1}{6}[2Br(\Xi+1)G_0 - BrG_1 - 2],$$
$$A_4 = \frac{1}{24}\{Br[2Br\Xi G_0^2 - 2(\Xi+1)(\Xi+3)G_0 + (4\Xi+3)G_1 - 2G_2] + 6\}, \ldots \tag{38}$$

Higher order coefficients can be obtained by applying iteratively the recursive relation Eq. (37). Then, the dimensionless velocity, the Nusselt number and the flow rate parameter are given by

$$u(r) = \frac{r^2}{r^2+M^2}\left[1 + \Xi \sum_{n=0}^{\infty} A_n (r-1)^n\right], \tag{39}$$

$$Nu = -\left[\sum_{n=0}^{\infty} A_n (\gamma-1)^n\right]^{-1}, \tag{40}$$

$$u_m = \frac{2}{\gamma^2-1}\left(B_0 + \Xi \sum_{n=0}^{\infty} A_n B_n\right), \tag{41}$$

where on account of Eq. (20), the coefficients B_n are defined as

$$B_0 = \frac{1}{2}\left[M^2 \ln\left(\frac{M^2+1}{M^2+\gamma^2}\right) + \gamma^2 - 1\right],$$
$$B_1 = \frac{1}{6}\left\{3M^2\left[2M \arctan\left(\frac{\gamma}{M}\right) - 2M \arctan\left(\frac{1}{M}\right) - \ln\left(\frac{M^2+1}{M^2+\gamma^2}\right)\right] - (\gamma-1)(6M^2-2\gamma^2+\gamma+1)\right\}, \ldots, B_n = \int_1^{\gamma} \frac{r^3(r-1)^n}{r^2+M^2}\,\mathrm{d}r. \tag{42}$$

3.3. The power series solution in the special case $\Xi \to \infty$

When the pressure gradient vanishes, *i.e.* $\mathrm{d}P/\mathrm{d}Z \to 0$, one has a flow driven only by buoyancy force and by MHD body force. In Section 3.1, this flow has been called MHD free convection regime. When $\mathrm{d}P/\mathrm{d}Z \to 0$ or $\Xi \to \infty$, one may infer that $t(r), u(r)/\Xi, Br\Xi^2, Nu$ and u_m/Ξ tend to a finite limit. The series solution procedure described in Section 3.2 can still be applied. Let us introduce the quantities

$$\Lambda = Br\Xi^2, \quad \tilde{u}(r) = \frac{u(r)}{\Xi}, \quad \tilde{u}_m = \frac{u_m}{\Xi}. \tag{43}$$

Then, when $\Xi \to \infty$, Eq. (30) simplifies to

$$rt''(r) + t'(r) + \Lambda G(r) t(r)^2 = 0. \tag{44}$$

It is easily shown that, in the limit $\Xi \to \infty$, one has

$$t(r) = \sum_{n=0}^{\infty} \tilde{A}_n (r-1)^n, \tag{45}$$

$$\tilde{u}(r) = \frac{r^2}{r^2+M^2} \sum_{n=0}^{\infty} \tilde{A}_n (r-1)^n, \tag{46}$$

$$Nu = -\left[\sum_{n=0}^{\infty} \tilde{A}_n (\gamma-1)^n\right]^{-1}, \tag{47}$$

$$\tilde{u}_m = \frac{2}{\gamma^2-1} \sum_{n=0}^{\infty} \tilde{A}_n B_n, \tag{48}$$

where the coefficients $\tilde{A}_n$ are evaluated through the relations

$$\tilde{A}_0 = 0; \quad \tilde{A}_1 = -1;$$
$$\tilde{A}_{n+2} = -\frac{n+1}{n+2}\tilde{A}_{n+1} - \frac{\Lambda}{(n+1)(n+2)} \sum_{j=0}^{n} G_{n-j} \left(\sum_{i=0}^{j} \tilde{A}_i \tilde{A}_{j-i} \right), \quad n \geqslant 2. \tag{49}$$

On account of Eq. (49), the coefficients $\tilde{A}_2, \tilde{A}_3$ and $\tilde{A}_4$ are given by

$$\tilde{A}_2 = \frac{1}{2}, \quad \tilde{A}_3 = -\frac{1}{3}, \quad \tilde{A}_4 = \frac{1}{12}(3 - \Lambda G_0), \ldots \tag{50}$$

3.4. Numerical solution

The initial value problem defined by Eqs. (15)–(17), can be also solved numerically by employing, for instance, Adams method, Euler's method or Runge–Kutta methods. A convenient environment for these numerical solution procedures is function `NDSolve` of software *Mathematica* (©Wolfram Research, Inc.). This function allows one to specify the desired method for the solution of the initial value problem or to accept the default optimal choice made by *Mathematica* kernel [21]. In the following, the numerical calculations are performed by choosing the predictor–corrector Adams method.

4. Discussion of the results

The results discussed in the following have been obtained either analytically or numerically through the function `NDSolve` of *Mathematica*. In the general case, the series solutions obtained in Sections 3.2 and 3.3 are used, by truncating the sums to the first 42 terms and adopting the Euler–Knopp algorithm for enhancing the convergence rate of the series [22]. This truncation ensures a satisfactory convergence in all the cases examined. A comparison between the analytical series solution and the numerical solution is performed in Table 1 with reference to $\gamma = 3, \phi = 0.5, Br = 1$, $M = 2$ and for different values of Ξ in the range $-0.6 \leqslant \Xi \leqslant 1.6$. The tested quantities are the dimensionless flow rate parameter

Table 1
Comparison between analytical and numerical solution: values of $u_m, Nu, \Delta u_m/u_m$ and $\Delta Nu/Nu$ versus Ξ, for $\gamma = 3, \phi = 0.5, Br = 1$ and $M = 2$

Ξ	u_m	Nu	$\Delta u_m/u_m$ (%)	$\Delta Nu/Nu$ (%)
−0.6	1.0703	0.28025	−0.0006	0.0053
−0.4	0.84300	0.34902	-3.0×10^{-5}	3.2×10^{-4}
−0.2	0.66578	0.42020	-4.8×10^{-7}	7.6×10^{-6}
−0.01	0.52880	0.48827	-9.2×10^{-11}	1.1×10^{-8}
0.01	0.51575	0.49538	3.1×10^{-11}	2.2×10^{-9}
0.2	0.40183	0.56162	2.7×10^{-10}	1.6×10^{-9}
0.4	0.29729	0.62698	3.6×10^{-9}	1.4×10^{-8}
0.6	0.20335	0.68496	4.9×10^{-8}	1.1×10^{-7}
0.8	0.11586	0.73236	8.1×10^{-7}	9.9×10^{-7}
1.0	0.031311	0.76590	2.6×10^{-5}	8.2×10^{-6}
1.2	−0.053577	0.78243	-1.2×10^{-4}	6.0×10^{-5}
1.4	−0.14218	0.77934	-3.0×10^{-4}	3.7×10^{-4}
1.6	−0.23834	0.75495	−0.0011	0.002

u_m and the Nusselt number Nu. In Table 1, the relative discrepancies between analytically and numerically obtained values

$$\frac{\Delta u_m}{u_m} = \frac{u_m[\text{analytical}] - u_m[\text{numerical}]}{u_m[\text{analytical}]}, \tag{51}$$

$$\frac{\Delta Nu}{Nu} = \frac{Nu[\text{analytical}] - Nu[\text{numerical}]}{Nu[\text{analytical}]}, \tag{52}$$

are determined. A very good agreement between analytical and numerical values of both u_m and Nu is found, the relative discrepancies being less than 0.0053%. In the table, it is clearly shown that the relative discrepancies $\Delta u_m/u_m$ and $\Delta Nu/Nu$ increase rapidly with $|\Xi|$. This is due to the loss of convergence rate of the power series for high values of $|\Xi|$. In the following analyses, both the numerical solution and the power series solution will be used to obtain and validate the results.

Table 1 shows that u_m is a monotonic decreasing function of Ξ, while Nu is a monotonic increasing function of Ξ. This behavior reflects the effect of the buoyancy force. The latter is directed downward at every position where the temperature is smaller than the reference temperature $T(R_1)$. In any case, every position in the porous layer has a temperature lower than the temperature of the internal boundary wall. In fact, even if internal heat generation is very intense, *i.e.* if Br is high, the maximum temperature always coincide with the reference value $T_{ref} = T(R_1)$.

The behavior of u_m shown in Table 1 reveals that, for positive values of Ξ, buoyancy tends to inhibit the upward average flow determined by the downward pressure gradient. Indeed, as stated above, the buoyancy force acts in the downward direction. The inhibition of upward flow, for sufficiently high positive values of $|\Xi|$, eventually produces an inversion of the average flow, from upward to downward. The latter feature, is shown by the negative values of u_m for $\Xi = 1.2, 1.4, 1.6$. A negative sign of u_m means that the average flow occurs in the direction of increasing hydrodynamic pressure P, as it can be easily inferred from Eq. (21).

4.1. The special case $\Xi \to \infty$

The limiting case $\Xi \to \infty$ corresponds to convective flow with vanishing axial pressure gradient ($dP/dZ \to 0$). In the preceding sections, this flow regime has been called MHD free convection regime. As it has been shown in Section 3.3, the governing parameters are in this case γ, ϕ, M and Λ.

Figs. 2 and 3 display plots of $t(r)$ and $\tilde{u}(r)$ with $\gamma = 3$ and $\phi = 0.5$ either for a fixed Λ (Fig. 2, $\Lambda = 3$) or for a fixed M (Fig. 3, $M = 2$). Fig. 2 shows that the dimensionless temperature differences tend to decrease as M increases. The dimensionless velocity at every position tends to become smaller and smaller as M increases and becomes zero (fluid at rest) in the limit $M \to \infty$. Fig. 3 displays the

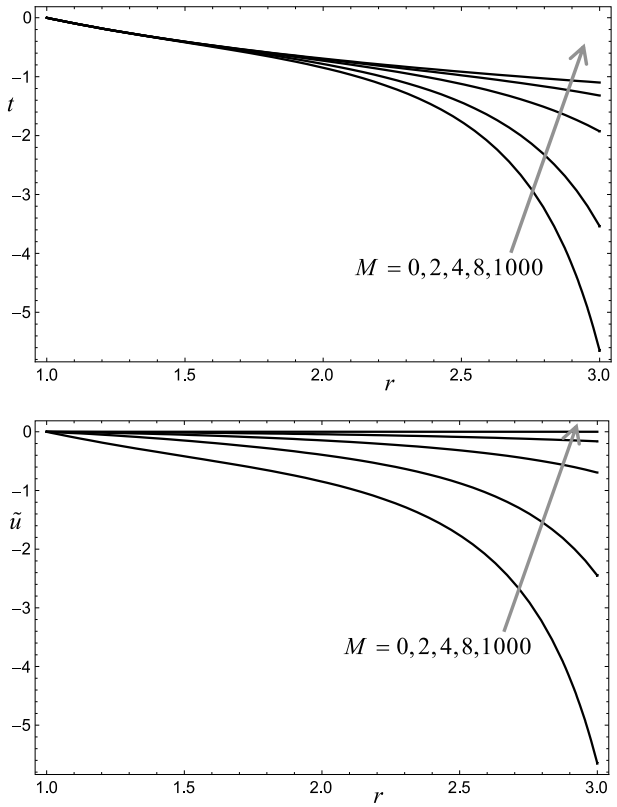

Fig. 2. Special case $\Xi \to \infty$: plots of $t(r)$ and $\tilde{u}(r)$ for $\gamma = 3, \Lambda = 3$ and $\phi = 0.5$.

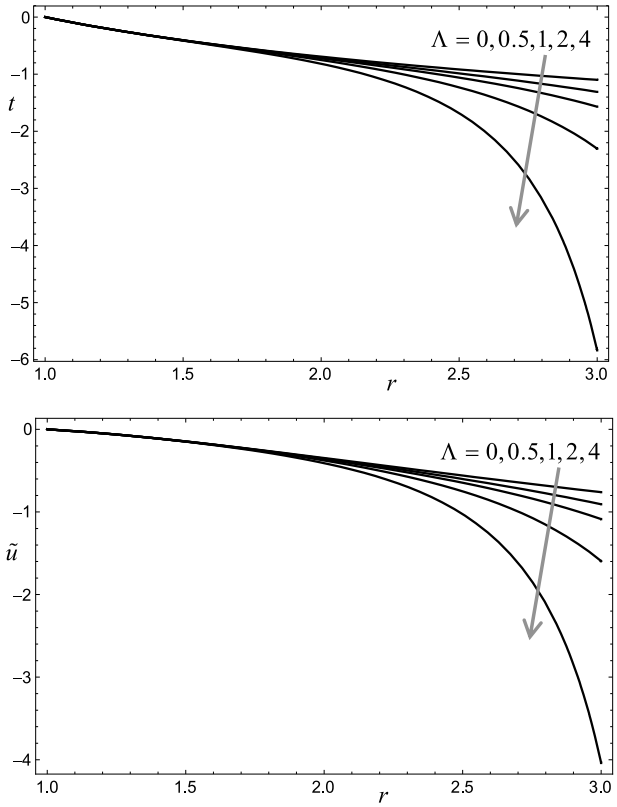

Fig. 3. Special case $\Xi \to \infty$: plots of $t(r)$ and $\tilde{u}(r)$ for $\gamma = 3, M = 2$ and $\phi = 0.5$.

effect of parameter Λ on the distributions $t(r)$ and $\tilde{u}(r)$. This figure clearly shows that the slopes of $t(r)$ and $\tilde{u}(r)$ at $r = 1$ are indepen-

dent of Λ. As it has been already stressed, the definition of t constrains $t(r)$ to have a fixed slope at $r = 1$ (see Eq. (16)). Eqs. (14)–(17) and (43) reveal that, in the limit $\Xi \to \infty$, also $\tilde{u}'(1)$ is independent of Λ, namely $\tilde{u}'(1) = -1/(1 + M^2)$.

Fig. 4 shows the change of parameters $\tilde{u}_m$ and Nu with M, for increasing values of Λ. This figure reveals that an increasing value of Λ, *i.e.* increasing effects of internal heat generation, implies decreasing values of both $\tilde{u}_m$ and Nu. In fact, a higher heat generation in the fluid produces larger temperature differences and, thus, yields smaller values of Nu and more intense buoyant downflow (smaller negative values of $\tilde{u}_m$). Fig. 4 shows once again the behavior when M becomes very large: flow is progressively inhibited and for $M \to \infty$ the fluid is at rest. For $\Lambda \to 0$, the dimensionless temperature distribution is given by the logarithmic profile $t(r) = -\ln(r)$; the Nusselt number is thus independent of M and has the value $Nu = 1/\ln(\gamma) = 1/\ln(3) \cong 0.910239$.

4.2. Combined effects of buoyancy and heat generation

In the general case, the parameters Br, Ξ and M have finite non-vanishing values. An example of this general condition is illustrated in Fig. 5 where plots of the dimensionless temperature t and of the dimensionless velocity u are reported for $\gamma = 3, \phi = 0.5$ and $M = 2$. The behavior of t and u is analyzed for different values of Br either in a case of upward hydrodynamic pressure force $-dP/dZ$ (the solid lines corresponding to $\Xi = 1$) or in a case of downward hydrodynamic pressure force (the dashed lines corresponding to $\Xi = -1$). Fig. 5 shows that the effect of the internal heat generation due to both Joule heating and viscous dissipation is stronger in the case of downward hydrodynamic pressure force ($\Xi = -1$). This result is apparent by inspecting the plots of dimensionless velocity and temperature. The physical reason is that, when $-dP/dZ > 0$, buoyancy tends to contrast the up-

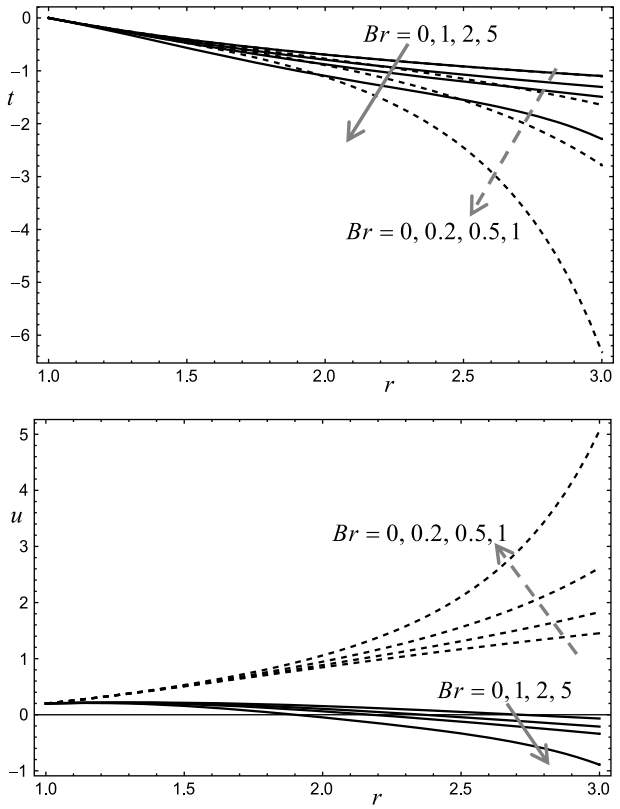

Fig. 5. Plots of $t(r)$ and $u(r)$ for $\gamma = 3, \phi = 0.5, M = 2$ and $\Xi = 1$ (solid lines) or $\Xi = -1$ (dashed lines).

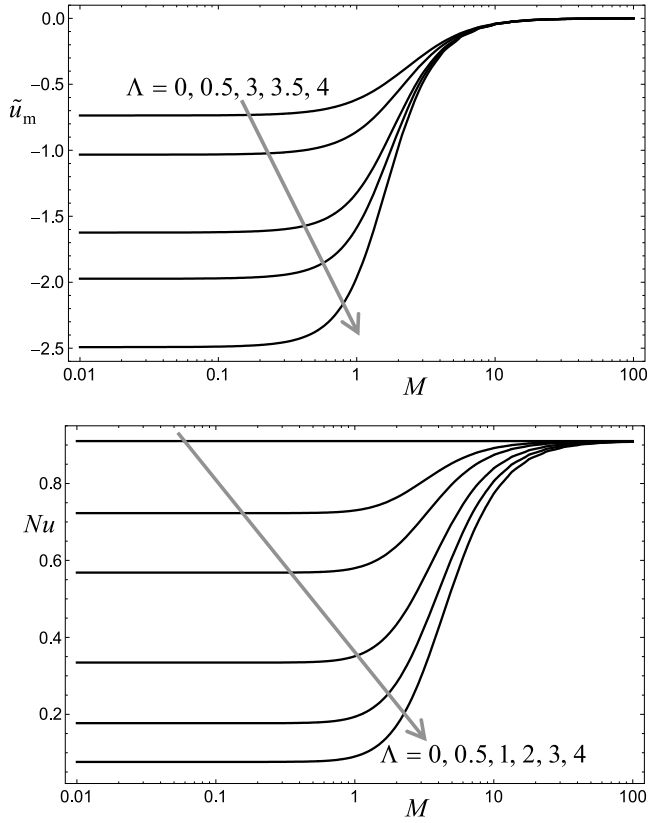

Fig. 4. Special case $\Xi \to \infty$: plots of $\tilde{u}_m$ and Nu versus M, for $\gamma = 3$, $\phi = 0.5$ and increasing values of Λ.

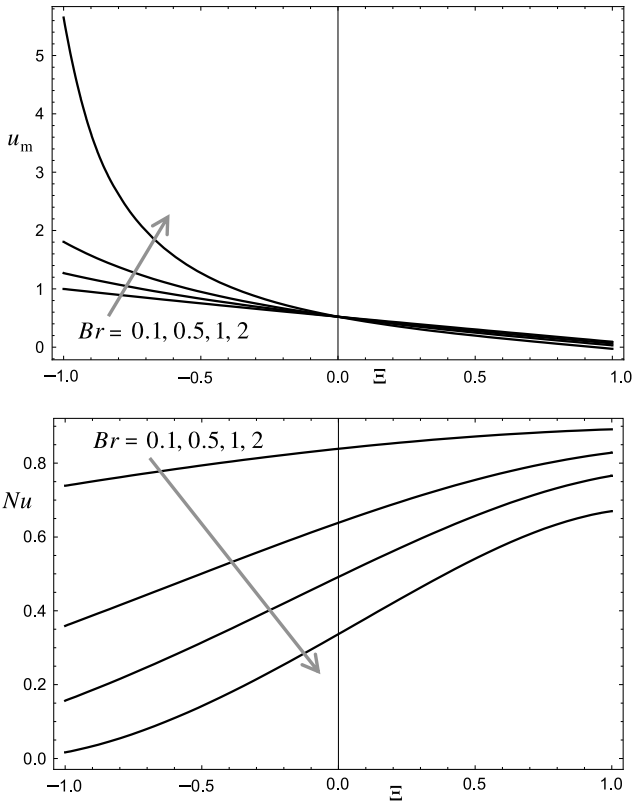

Fig. 6. Plots of u_m and Nu versus Ξ, for $\gamma = 3, \phi = 0.5, M = 2$ and increasing values of Br.

ward flow induced by the hydrodynamic pressure force. As a consequence, for a given value of $|U_{ref}|$ defined by Eq. (13), and hence of Br, one has a smaller effect of heat generation than in the case $-\mathrm{d}P/\mathrm{d}Z < 0$, due to the smaller local values of u^2. On the other hand, in the case $-\mathrm{d}P/\mathrm{d}Z < 0$, buoyancy and hydrodynamic pressure force act in the same downward direction.

The combined effect of buoyancy and internal heat generation on the Nusselt number Nu and the flow rate parameter u_m is illustrated in Fig. 6. This figure shows that u_m has an important dependence on Br only in the case of downward hydrodynamic pressure force ($\Xi < 0$). In this case, u_m is an increasing function of Br. Moreover, for $\Xi < 0, u_m$ is an increasing function of $|\Xi|$, *i.e.* downflow is enhanced by buoyancy. In other words, for $\Xi < 0$, buoyancy and internal heat generation act synergically in driving the fluid flow downward. It can be easily observed that, for $\Xi \to 0$, all the curves of u_m corresponding to different Br intersect with each other, since the dimensionless velocity is not influenced by Br in this limit (forced convection). Fig. 6 also shows that Nu is a decreasing function of Br. This behavior is a well known feature of internal convective flows under conditions of prescribed wall heat flux [23].

5. Conclusions

MHD mixed convection flow has been analyzed in an annular region filled with a fluid saturated porous medium. The annulus surrounds a cable carrying a stationary electric current that creates the magnetic field. Due to Biot–Savart law, the latter is a transverse field with a radially decreasing module. The internal boundary, *i.e.* the interface between the cable and the porous medium, has been assumed to be an isoflux wall, while the external boundary has been assumed to be isothermal. The fully developed regime has been considered and the velocity field has been assumed to be parallel. The momentum and energy balance equations have been written according to Darcy law and Boussinesq approximation, by taking into account both the effect of Joule heating and that of viscous dissipation. For fixed values of the radial aspect ratio and of the porosity of the solid matrix, the balance equations written in a dimensionless form contain three governing parameters: the Hartmann number M, the Brinkman number Br and the ratio $\Xi = Gr/Re$ between the Grashof number and the Reynolds number. The most important results obtained are the following.

- The buoyancy effect is analyzed by setting the fluid density next to the isoflux boundary wall as the reference density. In this way, the boundary value problem implied by the momentum and energy balance equations is in fact transformed into an initial value problem with a unique solution for any given set of values of the governing parameters.
- The magnetic field inhibits the fluid flow either in the case of downward hydrodynamic pressure force or in the case of upward hydrodynamic pressure force. As a consequence, the flow rate parameter u_m, proportional to the ratio between the average seepage velocity in a transverse cross-section and the hydrodynamic pressure force $-\mathrm{d}P/\mathrm{d}Z$, is a decreasing function of the Hartmann number. In the cases examined, no appreciable flow rate exists for $M \gtrsim 10$.
- In the limit $\Xi \to \infty$, no hydrodynamic pressure force acts on the fluid, so that flow is driven only by buoyancy and magnetic force (MHD free convection). In this limit, the average flow is downward. The downward flow rate increases as the effect of heat generation, due to both Joule heating and viscous dissipation, becomes more and more important.

It must be pointed out that the shape of the velocity and temperature profiles depend in general on the choice of the reference temperature T_{ref}. This is a common feature in the analysis of buoyant flows. By making a choice of T_{ref}, one defines exactly the constant pressure gradient $\mathrm{d}P/\mathrm{d}Z$. Different choices of T_{ref} unavoidably imply a different meaning of the condition $\mathrm{d}P/\mathrm{d}Z = 0$. As a direct inference, different choices of T_{ref} necessarily lead to a different definition of the MHD free convection regime, *i.e.* the limiting case $\Xi \to \infty$. Then, the conclusion that, when $\mathrm{d}P/\mathrm{d}Z = 0$, the average flow is downward obviously depends on the choice of T_{ref} as equal to the temperature on the isoflux boundary. A different choice of T_{ref} would have implied a different meaning of the condition of MHD free convection regime and, as a consequence, different flow features in this regime.

References

[1] D.A. Nield, A. Bejan, Convection in Porous Media, third ed., Springer, New York, 2006.
[2] A.J. Chamkha, A.-R.A. Khaled, Nonsimilar hydromagnetic simultaneous heat and mass transfer by mixed convection from a vertical plate embedded in a uniform porous medium, Numer. Heat Transfer, Part A 36 (1999) 327–344.
[3] M. Kumari, H.S. Takhar, G. Nath, Mixed convection flow over a vertical wedge embedded in a highly porous medium, Heat Mass Transfer 37 (2001) 139–146.
[4] A.J. Chamkha, M.M.A. Quadri, Heat and mass transfer from a permeable cylinder in a porous medium with magnetic field and heat generation/absorption effects, Numer. Heat Transfer, Part A 40 (2001) 387–401.
[5] M.A. Seddeek, Effects of magnetic field and variable viscosity on forced non-Darcy flow about a flat plate with variable wall temperature in porous media in the presence of suction and blowing, J. Appl. Mech. Tech. Phys. 43 (2002) 13–17.
[6] M.A. Mansour, N.A. El-Shaer, Effect of magnetic field on non-Darcy axisymmetric free convection in a power-law fluid saturated porous medium with variable permeability, J. Magn. Magn. Mater. 250 (2002) 57–64.
[7] M.F. El-Amin, Combined effect of magnetic field and viscous dissipation on a power-law fluid over plate with variable surface heat flux embedded in a porous medium, J. Magn. Magn. Mater. 261 (2003) 228–237.
[8] A. Postelnicu, Influence of a magnetic field on heat and mass transfer by natural convection from vertical surfaces in porous media considering Soret and Dufour effects, Int. J. Heat Mass Transfer 47 (2004) 1467–1472.
[9] D.S. Rakoto Ramambason, P. Vasseur, Influence of a magnetic field on natural convection in a shallow porous enclosure saturated with a binary fluid, Acta Mech. 191 (2007) 21–35.
[10] T. Hayat, M. Khan, S. Asghar, On the MHD flow of fractional generalized Burgers' fluid with modified Darcy's law, Acta Mech. Sinica 23 (2007) 257–261.
[11] M. Khan, C. Fetecau, T. Hayat, MHD transient flows in a channel of rectangular cross-section with porous medium, Phys. Lett. A 369 (2007) 44–54.
[12] T. Hayat, T. Javed, On analytic solution for generalized three-dimensional MHD flow over a porous stretching sheet, Phys. Lett. A 370 (2007) 243–250.
[13] B.S. Bhadauria, Magnetofluid convection in a rotating porous layer under modulated temperature on the boundaries, ASME J. Heat Transfer 129 (2007) 835–843.
[14] B.S. Bhadauria, Combined effect of temperature modulation and magnetic field on the onset of convection in an electrically conducting-fluid-saturated porous medium, ASME J. Heat Transfer 130 (052601) (2008) 9.
[15] O.G. Martynenko, P.P. Khramtsov, Free-Convective Heat Transfer, Springer, Berlin, 2005, pp. 4–5.
[16] B.R. Morton, Laminar convection in uniformly heated vertical pipes, J. Fluid Mech. 8 (1960) 227–240.
[17] D.A. Nield, Modeling the effects of a magnetic field or rotation on flow in a porous medium: momentum equation and anisotropic permeability analogy, Int. J. Heat Mass Transfer 42 (1999) 3715–3718.
[18] P.H. Roberts, An Introduction to Magnetohydrodynamics, Longman, London, 1967, pp. 3–4.
[19] K. Kaviany, Principles of Heat Transfer in Porous Media, second ed., Springer, Berlin, 1995, pp. 22, 28.
[20] A. Erdélyi, W. Magnus, F. Oberhettinger, F.G. Tricomi, Higher Transcendental Functions, vol. 1, McGraw-Hill, New York, 1953, p. 31.
[21] S. Wolfram, The Mathematica Book, fifth ed., Wolfram Media, 2003, pp. 978–979.
[22] K. Knopp, Theory and Application of Infinite Series, Dover, New York, 1990.
[23] R.K. Shah, A.L. London, Laminar Flow Forced Convection in Ducts. Advances in Heat Transfer, Suppl. 1, Academic press, New York, 1978, p. 82.